Lithuanian Journal of Physics, Vol. **46**, No. 1, pp. 33–38 (2006)

INVESTIGATION OF DYNAMIC CHARACTERISTICS OF InGaAsP / InP LASER DIODES

E. Šermukšnis [a], V. Palenskis [a], J. Matukas [a] S. Pralgauskaitė [a], J. Vyšniauskas [a], and R. Baubinas [b]

[a] *Radiophysics Departament, Vilnius University, Saulėtekio 9, LT-10222 Vilnius, Lithuania*
E-mail: emilis.sermuksnis@ff.vu.lt, vilius.palenskis@ff.vu.lt, jonas.matukas@ff.vu.lt, sandra.pralgauskaite@ff.vu.lt, juozas.vysniauskas@ff.vu.lt

[b] *Institute of Materials Science and Applied Research, Vilnius University, Saulėtekio 9, LT-10222 Vilnius, Lithuania*

Received 12 October 2005

We present the investigation results of dynamic characteristics for InGaAsP quantum-well lasers, where we look for the problems that have an influence on laser diode modulation speed, quality, and reliability. The experiments have shown that the investigated distributed feedback laser diodes have shorter turn-on delay time (from 0.6 ns to 1.2 ns) than Fabry–Perot lasers (from 0.8 ns to 1.4 ns). Different design samples have been investigated and it is found that the turn-on delay time increases with laser cavity length due to the active region volume increase. It is also shown that for the investigated structures the main carrier recombination mechanism is the non-radiative recombination through defects. The same defects have the main influence to the laser operation characteristic degradation during ageing.

Keywords: Fabry–Perot laser diodes, distributed feedback laser diodes, turn-on delay time, recombination mechanisms, reliability

PACS: 42.55.Px

1. Introduction

Semiconductor lasers are typical devices for information transmission in optical communication using direct modulation. Nowadays stable single-mode laser diodes (LDs) with a narrow linewidth, low chirp, and high speed modulation capability are highly desirable to prevent pulse variance in long-haul telecommunication systems [1–3]. Unfortunately, the communication system using a high-speed direct modulation is limited by transient (relaxation) oscillations that result from the interplay between the optical field and the carrier density [4–6].

The measurements of laser dynamic characteristics provide comprehensive information about their suitability for the particular application as well as give deeper understanding of device operation. The minimum turn-on delay time is a limiting factor for the laser modulation speed as it defines the maximal laser switching frequency. LD dynamic characteristics are determined by variations of the injected carriers density and emitted photon density in the active (and passive) region [7, 8]. As consequence, the carrier threshold density, lifetime, and prevailing recombination processes are important to know while labouring better performance (with lower non-radiative recombination and shorter turn-on delay time) LD structures.

In this paper, we present experimental and computational investigation results of dynamic characteristics for InGaAsP quantum-well lasers: turn-on delay time, threshold carrier density and threshold carrier lifetime, recombination parameters. The aim of investigation was to clear up the problems that influence the laser diode dynamic characteristics, their quality, and reliability.

2. Investigated devices

Investigated devices were the InGaAsP / InP Fabry–Perot (FP) and distributed feedback (DFB) multiple-quantum-well (QW) lasers radiating at 1.3 μm (FP LDs) and 1.55 μm (DFB LDs).

FP lasers were ridge waveguide ones containing ten 4 nm width QWs in the active region. FP LDs with different barrier layer energy band gap were investigated: barrier layer energy band gap changes from 1.03 eV to 1.24 eV. And cavity length of each type FP lasers ranged from 250 μm to 1000 μm.

ISSN 1648-8504

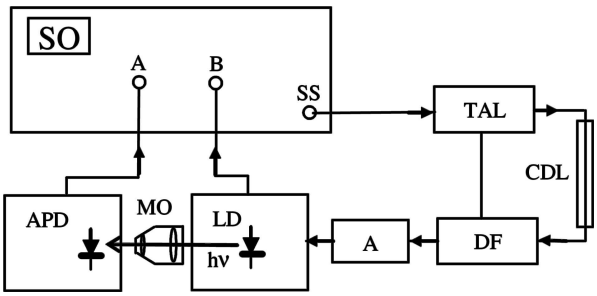

Fig. 1. Principle scheme for LD dynamic characteristic measurement: SO is sampling oscilloscope, TAL is transistor amplifier–limiter, CDL is coaxial delay line, DF is diode former, A is attenuator, LD is laser diode, APD is avalanche photodetector, A and B are inputs, SS is output of internal synchro-signal, MO is objective.

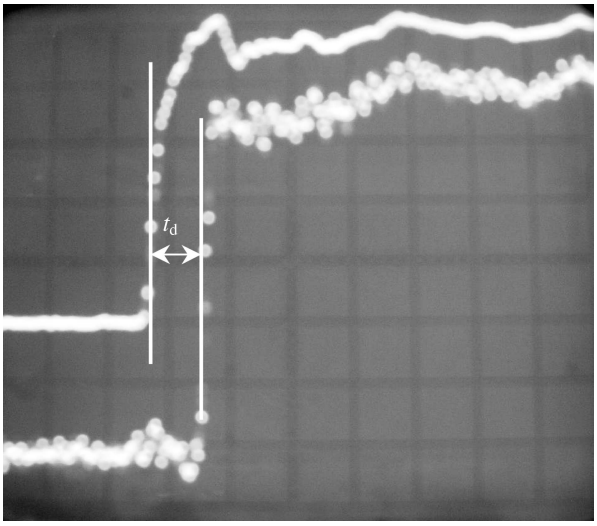

Fig. 2. Oscillograms for determination of turn-on delay time.

DFB lasers were buried heterostructures (BH) with active region containing 6 QWs. DFB samples cavity length was 300 μm.

3. Experimental set-up and modelling

Experimental investigation of laser diode dynamic characteristics meets some difficulties such as an observation and measurement of very short processes and metrological pulse quality. For the qualitative metrological pulse formation a sampling oscilloscope and a special signal former containing the transistor amplifier–limiter and diode former were used (Fig. 1). After the pulse formation the metrological pulse front was (0.10−0.15) ns. In Fig. 2, the oscillograms for determination of turn-on delay time are presented.

Dynamic LD characteristics are related with injected carrier and photon density variation in the active region. By approximating the experimental turn-on delay time dependences the carrier recombination parameters, threshold carrier density and lifetime can be evaluated. The injected carrier lifetime and photon lifetime at stable lasing conditions can be described by the rate equations [7, 8]

$$\frac{\mathrm{d}n}{\mathrm{d}t} = \frac{J}{qd} - \frac{n}{\tau_\mathrm{e}} - gn_\mathrm{ph}\,, \tag{1}$$

$$\frac{\mathrm{d}n_\mathrm{ph}}{\mathrm{d}t} = gn_\mathrm{ph} - \frac{n_\mathrm{ph}}{\tau_\mathrm{ph}} + \beta_\mathrm{sp}\frac{n}{\tau_\mathrm{e}}\,, \tag{2}$$

where n and n_ph are the densities of carriers and photons, τ_e and τ_ph are the injected carrier and photon lifetimes, respectively, g is the photon gain, β_sp is the spontaneous emission factor. The first term on the right hand side of Eq. (1) is the number of carriers injected per unit time and unit volume, the second term indicates the spontaneous emission, and the third term corresponds to the stimulated emission. In Eq. (2), the first term is the density of photons generated by stimulated recombination, the second is the density of photons lost from the cavity, and the third corresponds to the spontaneous emission.

While investigating LD below the lasing threshold the third term in Eq. (1) can be neglected [8]:

$$\frac{\mathrm{d}n}{\mathrm{d}t} = \frac{I}{qV} - \frac{n}{\tau_\mathrm{e}} = \frac{I}{qV} - n\gamma_\mathrm{e}(n)\,, \tag{3}$$

and turn-on delay time can be calculated from the following equation:

$$t_\mathrm{d} = qV\int\limits_{n_0}^{n_\mathrm{th}} \frac{1}{I - qV\gamma_\mathrm{e}(n)n}\,\mathrm{d}n\,, \tag{4}$$

where

$$\gamma_\mathrm{e}(n) = A + Bn + Cn^2\,, \tag{5}$$

is the recombination rate: the first right hand side term corresponds to the non-radiative recombination, the second term is the radiative interband recombination, and the third is the Auger recombination term. Carrier density without current pulse n_0 (at direct current I_0) and threshold carrier density n_th can be found from the initial conditions:

$$I_0 = qV\gamma_\mathrm{e}(n_0)n_0\,, \tag{6}$$

$$I_\mathrm{th} = qV\gamma_\mathrm{e}(n_\mathrm{th})n_\mathrm{th}\,. \tag{7}$$

Using Eqs. (4)–(7) and experimental turn-on delay time dependences, the recombination constants A, B, and C can be simulated and the influence of each recombination type can be evaluated. But approximation of Eq. (4) according to parameters A, B, and C is

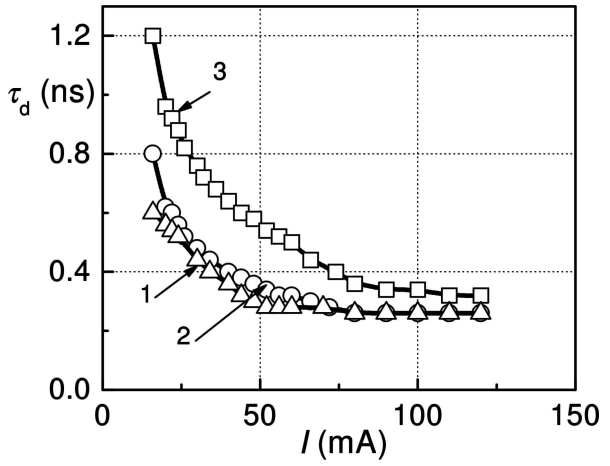

Fig. 3. Typical LD turn-on delay time dependences on pulse current at different direct currents: *1* at $I_0/I_{\rm th}$ = 0.32, *2* at $I_0/I_{\rm th}$ = 0.17, *3* at $I_0/I_{\rm th}$ = 0.02 (for DFB sample).

quite complicated because the approximation parameters are not only in the integrand function but also in the both limits of integration. Standard software does not contain such complex approximation tools. Therefore, the programme for our particular demands was written. When the dimensions of the LD active region, the threshold current $I_{\rm th}$, and the direct current I_0 are set, the programme picks out the parameters A, B, and C and calculates the turn-on delay time dependence on the pulse current. At approximation all three recombination types (non-radiative recombination through defects, radiative interband recombination, and Auger processes) are taken into account.

Using the calculated parameters A, B, and C the threshold carrier lifetime $\tau_{\rm e}$ and differential threshold carrier lifetime $\tau_{\rm e}'$ can be calculated from the equations (experimental measurement conditions must be $I_0 = 0$, $I \gg I_{\rm th}$) [8]:

$$\tau_{\rm e}(n_{\rm th}) = \left(A + Bn_{\rm th} + Cn_{\rm th}^2\right)^{-1}, \qquad (8)$$

$$\tau_{\rm e}'(n_{\rm th}) = \left(A + 2Bn_{\rm th} + 3Cn_{\rm th}^2\right)^{-1}. \qquad (9)$$

4. Results and discussion

The turn-on delay time was measured at room temperature and at different direct currents I_0, at different pulse currents. The turn-on delay time decreases with direct current and / or pulse current increase (Fig. 3). When the direct current is close to the threshold one, the turn-on delay time approaches its minimal value and practically does not depend on the pulse current. The behaviour of the turn-on delay time dependence on current is determined by the injected carrier density: at

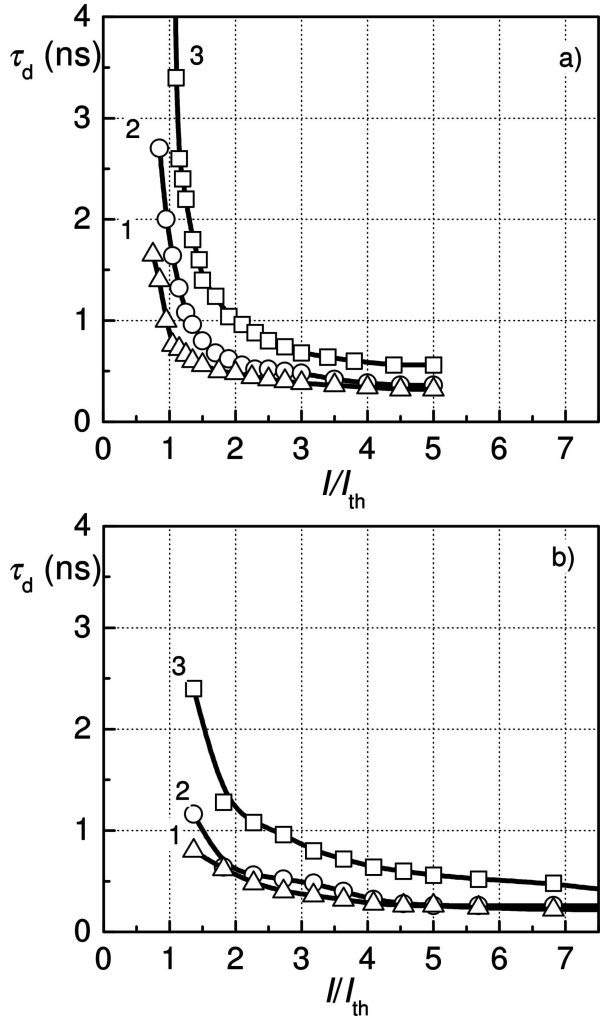

Fig. 4. Comparison of (a) FP (*1* at $I_0/I_{\rm th}$ = 0.381, *2* at $I_0/I_{\rm th}$ = 0.19, *3* at $I_0/I_{\rm th}$ = 0.01) and (b) DFB (*1* at $I_0/I_{\rm th}$ = 0.31, *2* at $I_0/I_{\rm th}$ = 0.16, *3* at $I_0/I_{\rm th}$ = 0.02) LD turn-on delay time dependences on pulse current amplitude.

larger direct current less carriers have to be injected by pulse current to reach the threshold carrier density and a larger pulse leads to a faster carrier injection into the active region. So, at larger direct and / or pulse currents less time is needed to achieve the stationary lasing operation.

At operation conditions when the direct current is much lower than the laser threshold current ($I_0/I_{\rm th} \approx 0.01$) and the pulse current exceeds the threshold one twice ($I = 2I_{\rm th}$), the investigated DFB LD turn-on delay time is in the range from 0.6 ns to 1.2 ns, while the FP laser turn-on delay time ranges from 0.8 ns to 1.4 ns (Fig. 4). As the turn-on delay time is strongly correlated with the lasing threshold conditions, the comparison of different samples turn-on delay times ignoring their threshold currents does not give particular information about the laser diodes operation capabilities and

quality. But comparison of the DFB and FP samples with a similar threshold current (e. g. $I_{\rm th}$ = 18 mA: delay time of FP sample 1.07 ns, of DFB sample – 0.74 ns; $I_{\rm th}$ = 26 mA: delay time of FP sample 1.45 ns, of DFB sample – 0.69 ns) shows that nevertheless the DFB laser operation is noticeably faster than the FP one. Two reasons of faster operation of the investigated DFB lasers can be noted. First, in the DFB LD optical spectrum there is only one gained mode (in FP LDs usually there are 6–8 main modes). Thus, a lower threshold carrier density (then a shorter time is needed for carriers to fill up the active region) is needed to reach the lasing threshold condition for one mode than for a batch of modes in a FP laser.

Furthermore, the investigated DFB LDs are buried heterostructure devices (while FP lasers are ridge waveguide diodes). BH lasers have current-blocking layers that strictly confine injected carriers in the active region and their operation characteristics (such as the threshold current, efficiency, modulation speed) are much better compared with the ridge waveguide LDs [9]. FP lasers with different cavity lengths have been investigated. The cavity length increase (from 250 to 1000 μm) leads to the active region volume increase and consequently the threshold current increase from the value of about 20 mA for 250 μm long samples to (60−90) mA for 1000 μm ones, i. e. the threshold current is approximately proportional to the channel length: to achieve the same carrier density for longer channel a larger current is needed because the cross-section of the active region is the same. The measurement results have completely confirmed this assumption, only a weak tendency, about (10−20)%, of decrease of slope efficiency $\mathrm{d}P/\mathrm{d}I$ for long (1000 μm) LDs is observed. This is related with the increased losses in cavity for long channels.

FP laser diodes with different barrier layer band gap were investigated, too, but the influence of the barrier layer due to band gap changes on the turn-on delay time was not found.

Laser diode reliability was investigated by examining the samples before and after an accelerated ageing (ageing conditions: 150 mA direct current at 130 °C during 3000 h). During ageing for some of the investigated LDs the operation characteristics degraded: the threshold current increased (from 8 to 27 mA), and the slope efficiency decreased. The turn-on delay time for those samples increased from 0.25 ns before ageing to 0.45 ns after ageing (at $I = 2I_{\rm th}$ and $I_0/I_{\rm th} \approx 0.1$; Fig. 5).

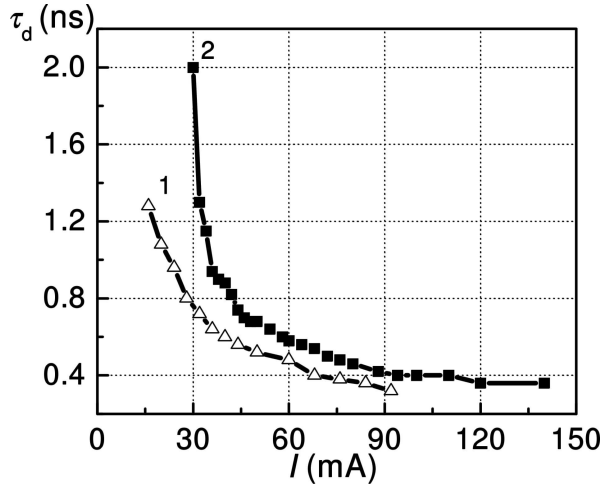

Fig. 5. DFB LD turn-on delay time dependence on pulse current for sample without ageing (curve *1*) and after ageing for 3000 h (curve *2*). I_0 = 0.2 mA.

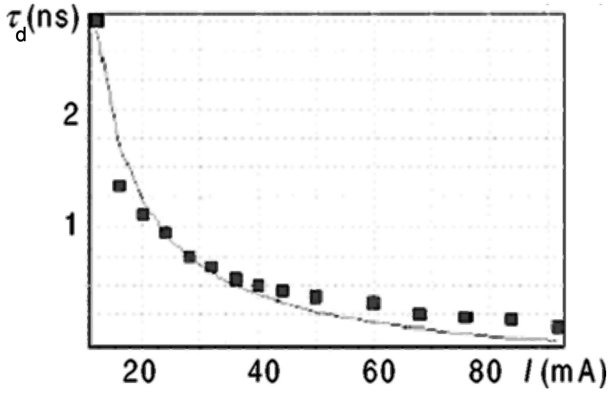

Fig. 6. The turn-on delay time dependence on the pulse current: squared dots are the experimental data, solid line is a theoretical approximation. I_0 = 0.2 mA.

The experimental turn-on delay time dependences were approximated theoretically (Fig. 6), and the recombination parameters and the threshold characteristics were found. The evaluated recombination parameters indicate that the carrier recombination through defects has the main influence to the LD operation quality: for the investigated lasers before ageing the parameter A (corresponding to the non-radiative recombination rate) is in the range of $(7-8)\cdot 10^6$ cm/s, while after ageing it increases to the values of $(2-4)\cdot 10^8$ cm/s (parameters B and C, corresponding to the radiative interband and Auger recombination, are similar for all the investigated samples: $B = (10^{-11}-10^{-13})$ cm^3/s, $C = (1-5)\cdot 10^{-29}$ cm^6/s). Due to non-radiative recombination rate increase the threshold carrier density increases and carrier lifetime decreases: $n_{\rm th} = (2.6-3.3)\cdot 10^{18}$ cm^3 and $\tau_{\rm e}$ = (2.2−2.5) ns for lasers

without ageing, and $n_{\rm th}$ = (3.6−4.8)·10^{18} cm^3 and $\tau_{\rm e}$ = (1.0−1.9) ns after ageing.

Investigated LD characteristic degradation during ageing is related with defects acting as carrier capture centres, with their number increase, and due to their migration. Especially assailable are the interfaces between the active region and burying layers. Microscopic investigations of surfaces of cleaved ends of the investigated lasers showed that there are clearly seen defects at the active region and burying layers interface that form current leakage channels. As the number of defects increases, the larger part of injected carriers quickly recombine (leak out of the active region) through defects (short lifetime) and so a larger carrier density is needed to reach the laser threshold condition.

5. Conclusions

The dynamic characteristics of InGaAsP / InP quantum-well laser diodes (LDs) have been investigated experimentally and theoretically. The investigated distributed feedback (DFB) lasers have better modulation speed compared with Fabry–Perot (FP) ones: turn-on delay time for DFB lasers is in the range from 0.6 ns to 1.2 ns, while for FP LDs it is from 0.8 ns to 1.4 ns at a pulse current $I_0/I_{\rm th}$ = 2.

With an increasing laser diode channel length the threshold current increases proportionally to it, i. e. the lasing starts at the same current density. The changes of the barrier layer band gap do not have influence on the investigated lasers dynamic characteristics.

The theoretical approximation of the turn-on delay time dependence on pulse current has shown that the non-radiative recombination through defects is the most intensive recombination process in the investigated laser structures.

During ageing the investigated laser operation characteristics degrade due to macrodefect formation and migration. These defects lead to the carrier leakage out from the active region and consequently to the shorter carrier lifetime, to the larger threshold carrier density, and as a result to the longer turn-on delay time.

Acknowledgement

This work has been partly funded by the Lithuanian State Science and Studies Foundation (contract No. C-33 / 2005).

References

[1] J.M. Buldu, J. Garcia-Ojalvo, and M.C. Torrent, Demultiplexing chaos from multimode semiconductor lasers, IEEE J. Quantum Electron. **41**, 164–170 (2005).

[2] H.D.I. Abarbanel, M.B. Kennel, L. Illing, S. Tang, H.F. Chen, and J.M. Liu, Synchronization and communication using semiconductor lasers with optoelectronic feedback, IEEE J. Quantum Electron. **37**, 1301–1311 (2001).

[3] E. Šermukšnis, J. Vyšniauskas, V. Palenskis, J. Matukas, and S. Pralgauskaitė, Dynamic characteristics of gain-coupled InGaAsP laser diodes and their reliability, Kwartalnik elektroniki i telekomunikacji **50**, 591–603 (2004).

[4] E. Šermukšnis, J. Vyšniauskas, T. Vasiliauskas, and V. Palenskis, Computer simulation of high frequency modulation of laser diode radiation, Lithuanian J. Phys. **44**, 415–420 (2004).

[5] J. Paul, M.W. Lee, and K.A. Shore, 3.5-GHz signal transmission in an all-optical chaotic communication scheme using 1550-nm diode lasers, IEEE Photon. Technol. Lett. **17**, 920–921 (2005).

[6] J. Paul, M.W. Lee, and K.A. Shore, Effect of chaos pass filtering on message decoding quality using chaotic external-cavity laser diodes, Opt. Lett. **29**, 2497–2499 (2004).

[7] M. Fukuda, *Optical Semiconductor Devices* (John Willey & Sons, New York, 1999).

[8] G.P. Agrawal, *Semiconductor Lasers* (Van Nostrand Reinhold, New York, 1993).

[9] N. Yamamoto, S. Seki, Y. Noguchi, and S. Kondo, Design criteria of 1.3-μm multiple-quantum-well lasers for high-temperature operation, IEEE Photon. Technol. Lett. **12**, 137–139 (2000).

InGaAsP / InP LAZERINIŲ DIODŲ DINAMINIŲ CHARAKTERISTIKŲ TYRIMAS

E. Šermukšnis, V. Palenskis, J. Matukas, S. Pralgauskaitė, J. Vyšniauskas, R. Baubinas

Vilniaus universitetas, Vilnius, Lietuva

Santrauka

Išsamiai ištirtos Fabri ir Pero (FP) ir paskirstyto grįžtamojo ryšio (PGR) InGaAsP lazerinių diodų (kurių spinduliuotės bangos ilgis atitinkamai buvo 1,3 ir 1,55 μm) su daugeliu kvantinių duobių aktyviojoje srityje dinaminės charakteristikos, išanalizuotos lazerinių diodų moduliacijos spartą, kokybę ir ilgalaikiškumą ribojančios priežastys. FP lazeriniai diodai su keteriniu bangolaidžiu turėjo 10 kvantinių duobių, kurių kiekvienos plotis lygus 4 nm, barjerinių sluoksnių draudžiamųjų energijų tarpas kito nuo 1,03 eV iki 1,24 eV, o LD kanalo ilgis – nuo 250 iki 1000 μm. PGR lazerinių diodų aktyvioji sritis, kuri turėjo 6 kvantines duobes, buvo izoliuota įvairiatarpėmis pn sandūromis, o kanalo ilgis lygus 300 μm. Parodyta, kad PGR lazerinių diodų įsijungimo vėlavimo trukmė (0,6–1,2 ns) yra trumpesnė nei FP lazerinių diodų (0,8–1,4 ns). Ištyrus FP lazerinius diodus su skirtingais kanalo ilgiais, pastebėta, kad, didėjant LD kanalo ilgiui, ilgėja ir lazerinės generacijos įsijungimo vėlavimo trukmė; be to, šis trukmės padidėjimas yra proporcingas kanalo ilgiui, t. y. lazerinė generacija prasideda esant apytiksliai tam pačiam ilginiam srovės tankiui. Nustatyta, kad FP LD lazerinės generacijos įsijungimo vėlavimo trukmė beveik nepriklauso nuo barjerinių sluoksnių draudžiamosios energijos tarpo. Parodyta, kad pagrindinis tirtų lazerinių diodų krūvininkų savaiminės rekombinacijos mechanizmas yra nespinduliuojamoji rekombinacija defektuose: kuo didesnis defektų tankis, tuo mažesnė krūvininkų savaiminės rekombinacijos trukmė, tuo didesnis ir LD slenkstinės srovės tankis. Paspartintai pasendinus LD, pastebėta, kad kai kurių LD charakteristikų blogėjimą, o ypač jų lazerinės generacijos įsijungimo vėlavimo trukmės padidėjimą taip pat lemia defektai. Sendinimo metu didėja defektų kiekis, o dėl jų migracijos susidaro jų sankaupos (makrodefektai).